

## Investigating the effect of nano-silica on efficiency of the foam in enhanced oil recovery

Seyyed Ahmadreza Amirsadat\*, Babak Moradi\*\*,\*\*\*, Ali Zeinolabedini Hezave\*\*\*\*,†, Siamak Najimi\*, and Mehdi Hojjat Farsangi\*

\*Department of Petroleum Engineering, Science and Research Branch, Islamic Azad University, Tehran, Iran

\*\*School of Chemical Engineering, Faculty of Engineering, University of Tehran, Tehran, Iran

\*\*\*National Iranian Oil Company, Tehran, Iran

\*\*\*\*Fanavari Atiyeh Pouyandegan Exir Company, Incubation Centre of Science and Technology Park, Arak, Iran

(Received 26 February 2017 • accepted 5 September 2017)

**Abstract**—Due to the vast production of crude oil and consequent pressure drops through the reservoirs, secondary and tertiary oil recovery processes are highly necessary to recover the trapped oil. Among the different tertiary oil recovery processes, foam injection is one of the most newly proposed methods. In this regard, in the current investigation, foam solution is prepared using formation brine, C<sub>19</sub>TAB surfactant and air concomitant with nano-silica (SiO<sub>2</sub>) as foam stabilizer and mobility controller. The measurements revealed that using the surfactant-nano SiO<sub>2</sub> foam solution not only leads to formation of stable foam, but also can reduce the interfacial tension mostly considered as an effective parameter for higher oil recovery. Finally, the results demonstrate that there is a good chance of reducing the mobility ratio from 1.12 for formation brine and reservoir oil to 0.845 for foam solution prepared by nanoparticles.

Keywords: Surfactant Foam, Interfacial Tension, Foam Stability, Nano-silica Dioxide, Enhanced Oil Recovery, Mobility Ratio

### INTRODUCTION

Enhanced oil recovery (EOR) methods are developed to increase the oil recovery by improving the sweep efficiency [1] through reducing the mobility ratio and tendency of fingering. Among the different possible EOR methods, foam injection is one of the promising techniques to recover residual/trapped oil [2,3]. Foam is a two-phase system in which gas bubbles are enclosed by a thin liquid film while gas flow is easily controlled, and the volumetric sweep efficiency is improved [4].

Foam is usually unstable both thermodynamically and kinetically, especially under reservoir conditions; therefore, attention has been shifted towards finding suitable stabilizer agents for foam injection processes. Accordingly, and in light of the developments in the area of nano-technology, nanoparticles have received much attention as foam stability enhancer for EOR purposes [5-7]. On the other hand, existence of surfactants can reduce the surface tension, which means higher amounts of oil can be displaced by capillary pressure and injected fluid (surfactant foam) [8]. Not only is the foam injection process enabling reducing the surface tension and enhancing the oil recovery, but also controlling gas mobility in oil reservoirs, leading to higher oil recovery. After the gas injection, there is still considerable amount of oil remaining in the complex network of the pores, since it was not swept completely from the reservoir. One of the reasons behind this phenomenon, outlined by Glatz, is the unfavorable mobility ratio. Mobility ratio is defined as the ratio of mobility ( $\lambda$ ) of the displacing fluid (water) to the mobil-

ity of the displaced fluid (oil), where mobility is permeability ( $\kappa$ ) divided by viscosity ( $\mu$ ):

$$M = \frac{\lambda_{water}}{\lambda_{oil}} = \frac{\kappa_{water} / \mu_{water}}{\kappa_{oil} / \mu_{oil}} \quad (1)$$

Thus, there is an inverse relation between the volumetric sweep efficiency and the mobility ratio. A value of M greater than 1 is unfavorable because this will cause the instability of the displacement process, the so-called “viscous fingering” effect. Under the condition of a large viscosity difference between the displacing (water, lower viscosity) and displaced (oil, higher viscosity) fluids, the mobility ratio will become larger than one, and thus poor recovery will be reached. The fingering effect is highly undesirable as it promotes itself more and more, which sharply reduces the production as soon as the finger reaches the production well site. In an endeavor to decrease the mobility ratio below one, it is possible to use techniques increase the viscosity of displacing fluid. This helps to promote the displacing fluid in a stable, uniform manner and decrease the chance of fingering effect, thus increasing the efficiency of oil recovery.

Considering this fact, foam injection concomitant with stabilizers is proposed to control the gas mobility and improve the sweep efficiency by increasing the effective viscosity and decreasing the relative permeability of the gas [9-11]. Applying this proposed method, Zargartalebi et al. [11] studied the capability of hydrophilic and slightly hydrophobic silica nanoparticles to improve surfactant performance. Their study showed that the interfacial tension between nanoparticle-augmented surfactant solution and oil followed a rapid decrease in low surfactant concentrations, while it experienced an increase at higher concentrations [11]. Kim et al. [12] studied the dispersion stability and transport of silica nanoparticle in sand-pack whose surface coating was designed so that it could

†To whom correspondence should be addressed.

E-mail: zeinolabedinihezave.ali@gmail.com

Copyright by The Korean Institute of Chemical Engineers.

**Table 1. Formation brine analysis**

D (kg/l)	PH	Cond ( $\mu$ s)	T.D.S (ppm)	NaCl (ppm)	Cl <sup>-</sup> (ppm)	Na (ppm)	Ca <sup>2+</sup> (ppm)	Mg <sup>2+</sup> (ppm)	HCO <sub>3</sub> <sup>-</sup> (ppm)
1.045	7.5	95000	74000	64350	39050	25300	3500	1700	64

provide steric stabilization even at very high salinities. Their results revealed that an increase in calcium and nanoparticle concentrations at constant pH of 8.5 might lead to aggregation of the nanoparticles. At concentrations higher than 1% both for calcium and nanoparticles, highly viscous nanoparticle aggregates were generated and retained in the unconsolidated sand-pack whenever there was insufficient hydrodynamic force [13]. Sun et al. [13] demonstrated that the dynamic surface tension of SiO<sub>2</sub> dispersion without SDS led to a slight change in IFT. They also reported that the surface tension of SiO<sub>2</sub>/SDS solution was higher than that of pure SDS solution when SDS concentration was above 0.02 wt%. This observed trend can be related to this phenomenon that as the surfactant molecules adsorb on nanoparticles through hydrophobic interaction, the amount of SDS at air-water interface decreases.

To the best of our knowledge, no application of C<sub>19</sub>TAB as foaming agent has been hitherto reported in the literature. Herein, the effect of hexadecyltrimethylammonium bromide [CH<sub>3</sub>(CH<sub>2</sub>)<sub>15</sub>N(Br)(CH<sub>3</sub>)<sub>3</sub>] (C<sub>19</sub>TAB) concomitant with SiO<sub>2</sub> nanoparticles was examined on the foam stability of oil emulsion, IFT reduction and oil recovery using sand-pack flooding.

## MATERIALS AND METHODS

### 1. Formation Brine

For all the experiments, the prepared synthetic formation brine was utilized based on the formation brine analysis (see Table 1).

### 2. Crude Oil

The used crude oil was kindly supplied by National Iranian South Oil Co. (NISOC Co.) from one of the southern Iranian oilfields (see Table 2).

### 3. Surfactant

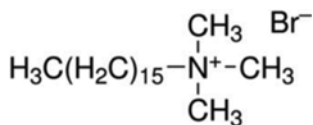
In the current investigation, hexadecyltrimethylammonium bromide [CH<sub>3</sub>(CH<sub>2</sub>)<sub>15</sub>N(Br)(CH<sub>3</sub>)<sub>3</sub>] (C<sub>19</sub>TAB) was supplied from Merck, Germany (Purity >99.9%) and used as model surfactant to stabilize the foam (see Fig. 1).

### 4. Silica (SiO<sub>2</sub>) Nanoparticles

The nanoparticles of silica (SiO<sub>2</sub>) (purity >99%), with mean par-

**Table 2. Crude oil properties**

Density (kg/l)	0.86
API <sup>o</sup>	33
Asphaltene (wt%)	6
Resin (wt%)	10

**Fig. 1. The structure of C<sub>19</sub>TAB.**

ticle size of 15-20 nm, were supplied from Sigma Aldrich, Germany.

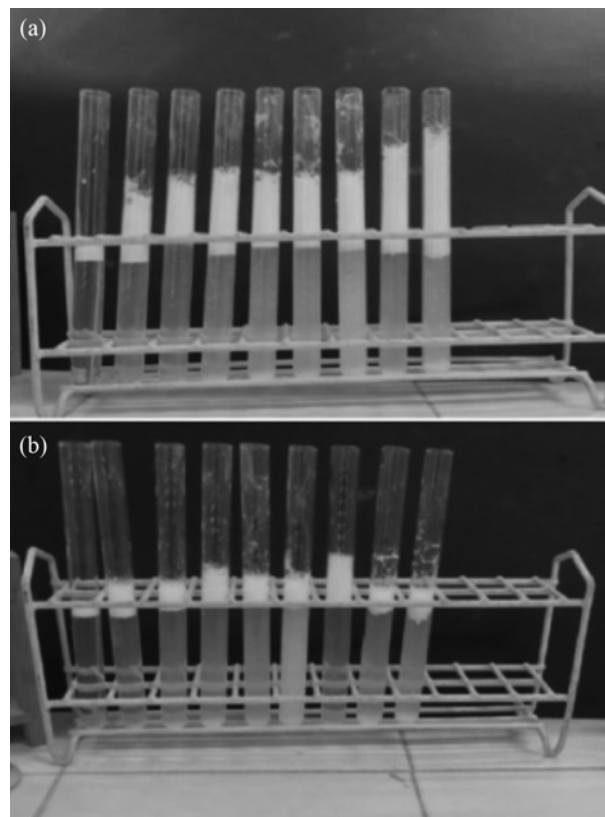
### 5. Foam Stability

As mentioned, one of the crucial and vital parameters during the foam injection is the solution stability [15]. Thus, a systematic series of experiments were designed to examine the effect of surfactants and surfactant/nanoparticles on stability of foam solution (see Fig. 2).

As can be seen in Figs. 2 and 3, the foam prepared with solutions containing no nanoparticles disappeared after 90 minutes after preparation, while the foam solutions prepared with nanoparticles were stable for about one month.

### 6. IFT Measurement

Generally, there are different methods for IFT measurements in liquid-liquid and liquid-gas systems. Due to the outweighing advantages of pendant drop method over other different available IFT measurement techniques, it has been used widely because of its capability to measure the IFT values at reservoir pressures and temperatures. In fact, the pendant drop shape method (the ADSA technique) is used for the measurement of the dynamic and equilibrium interfacial tension (DIFT and EIFT) [16,17]. A schematic diagram

**Fig. 2. Foam stability experiments, (a) at the start and (b) after 5,400 seconds (90 min) (C<sub>19</sub>TAB concentration changes from 100, 200, 500, 750, 1,000, 2,000, 3,000, 5,000 and 7,000 ppm (left to right)).**

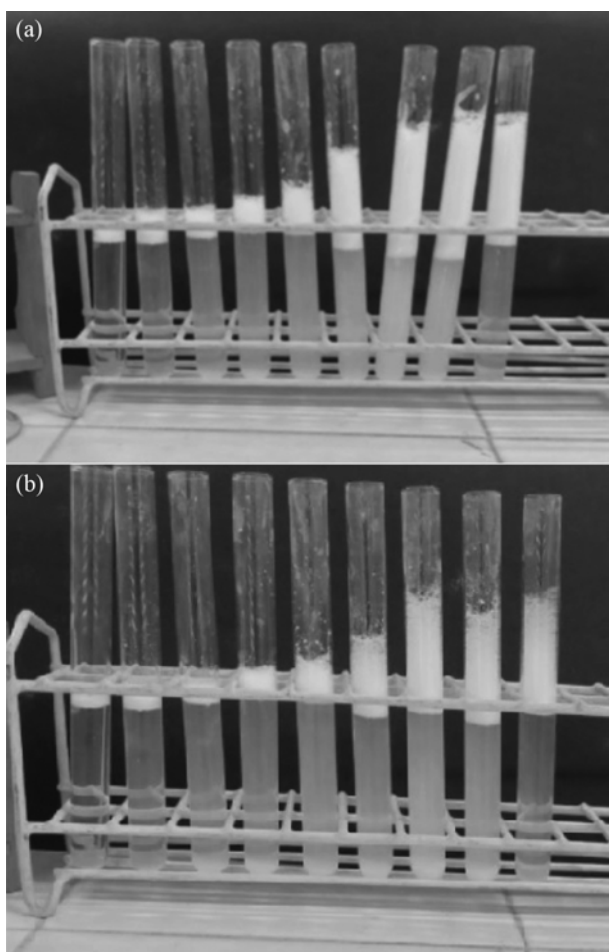


Fig. 3. Foam stability with constant concentration of SiO<sub>2</sub> nanoparticles of 500 ppm, (a) at the start and (b) after 12 h (CTAB concentrations 100, 200, 500, 750, 1,000, 2,000, 3,000, 5,000 and 7,000 ppm (left to right)).

of the equipment used is shown in Fig. 4. Actually, the basic parts of this apparatus consist of a high-temperature-high-pressure-optical cell made of stainless steel with inside injection needle that can be positioned downward or upward depending upon the density difference between the drop and bulk phases, and HP-HT sight glasses in front of each other that let light pass through the visual cell and the video tracking system, which captures the drop image. The video system was comprised of one CCD camera and one macro zoom Computar (Japan) lens. The output of the video system was analyzed by professional software installed on a personal computer (PC). To increase experimental results accuracy, the optical cell was fixed on a vibration-free platform to introduce stable and pronounced drop profiles. There was also one especially designed stainless steel cube equipped with two separated chambers, which can control the temperature of the system using three different slim heating elements and a PT-100 thermocouple. Each chamber was equipped with a moveable piston, holding CO<sub>2</sub> gas and crude oil sample to be injected via a manual handle pump. There were different valves installed on this equipment, which let the operator control the injection patterns of the drop and bulk phases described in detail elsewhere [16-21].

Finally, the point of each measurement was the average of five independent IFT measurements, which made it possible to calculate the uncertainties of the measurements and evaluate the repeatability of the measurements.

Using IFT measurement, it is possible to find the critical micelle concentration (CMC), which is one of the most important parameters defined as the surfactant concentration upon which the micelles will be spontaneously formed if the surfactant concentration exceeds this value. At CMC, further addition of surfactants leads to no significant change in the IFT value (see Fig. 5). Thus, before reaching CMC, the surface tension decreases sharply with the concentration of the surfactant, while its variation stops or slightly changes after reaching the CMC value [22].

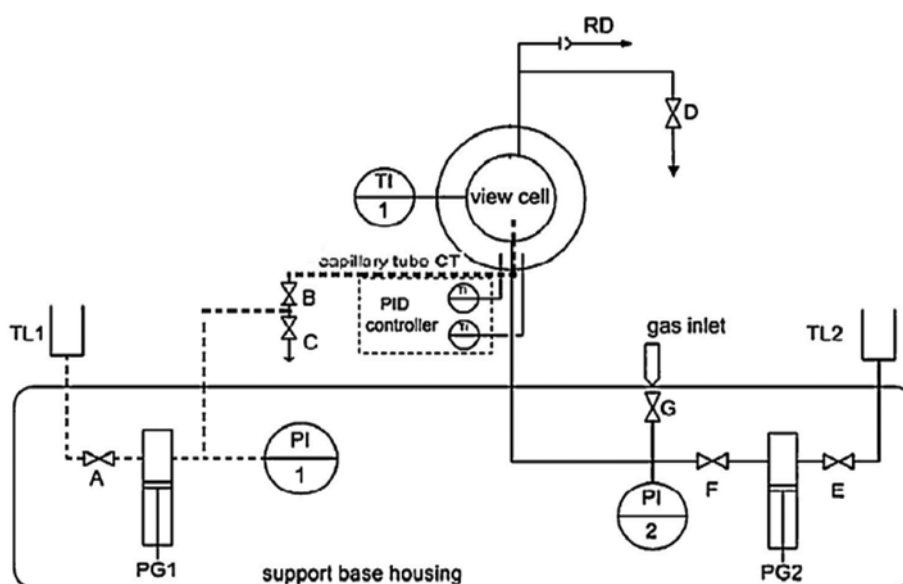


Fig. 4. Schematic of IFT apparatus: pressure generators (PG1 and PG2); temperature and pressure indicator (TI and PI), consisting of a thermocouple; rupture disk (RD); supply tanks for fluids (TL1, TL2); capillary tubes (CT) and dosage of liquid for pendant drop [17].

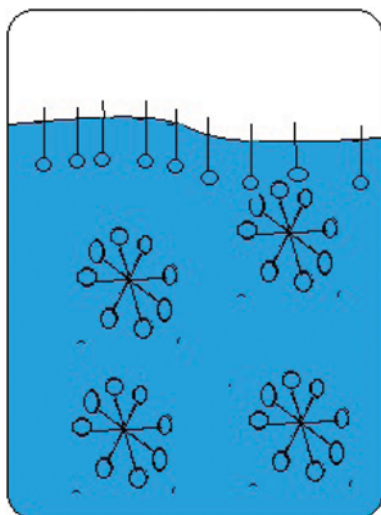


Fig. 5. Distribution of surfactant molecules in solution at concentrations above CMC.

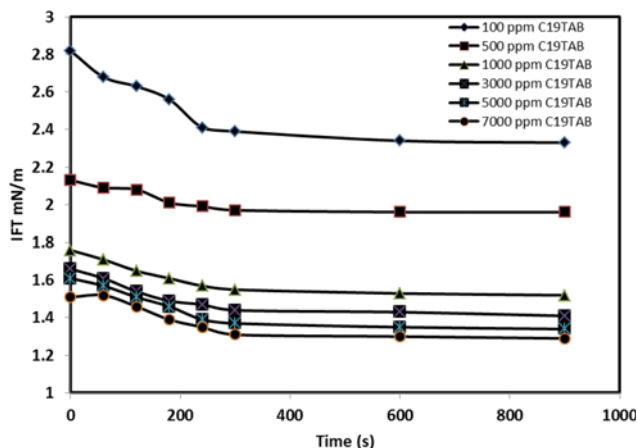


Fig. 6. Dynamic interfacial tension between crude oil and  $C_{19}TAB$  foam solution as a function of surfactant concentration.

## RESULTS AND DISCUSSION

### 1. IFT Measurement

In the first stage of this study, the IFT values were measured between crude oil and foam solutions containing different concentrations of  $C_{19}TAB$ . Accordingly, foam solutions were prepared by  $C_{19}TAB$  concentrations of 100, 500, 1,000, 3,000, 5,000 and 7,000 ppm (see Figs. 6 and 7). A closer examination of these figures revealed that the drops were stable for 900 s.

In addition, Fig. 6 shows that the CMC value of the examined systems is about 1,000 ppm of  $C_{19}TAB$ , meaning that no significant IFT changes would be observed for concentrations higher than 1,000 ppm. Thus, the concentration of 1,000 ppm was considered as the optimum concentration for the rest of the experiments.

### 2. Effect of $SiO_2$ Nanoparticles on IFT

At the next stage of this investigation, the effect of  $SiO_2$  nanoparticles concentration (0-1,000 ppm) was investigated on the IFT

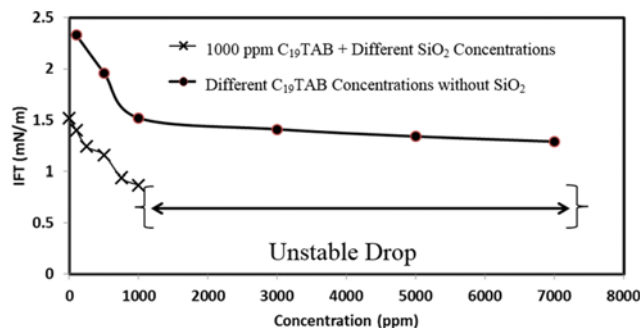


Fig. 7. IFT between crude oil and foam solutions.

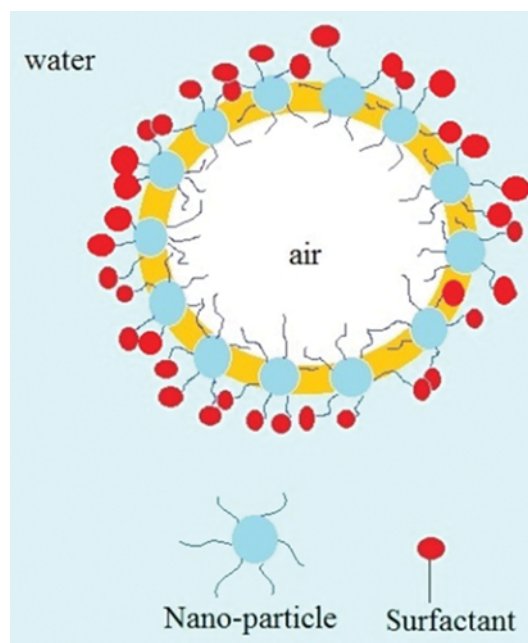


Fig. 8. Scheme: Nano-particles adsorption on gas-liquid film surface.

values between crude oil and foam solutions while the temperature was kept constant at  $75^\circ C$  (see Fig. 7). Fig. 7 shows that the IFT of crude oil/foam solution is a strong function of nano- $SiO_2$  concentration. Such an observation can be attributed to the adsorption of nanoparticles on the surface of gas-liquid film, which may lead to the generation of stable surfactant foam (see Fig. 8). On the other hand, the obtained results revealed that further increase in concentration from 750 ppm to 7,000 ppm led to no significant change on IFT, meaning that 750 ppm of  $SiO_2$  nanoparticle might be considered as the optimum concentration.

### 3. Mobility Control

As mentioned, mobility control is one of the most important concepts in any enhanced oil recovery process. In the foam injection process, it is possible to achieve the desired mobility ratio through injection of foams, which changes displacing fluid viscosity or preferentially reduces specific fluid relative permeability through injection of foams, which modifies wettability. The well-accepted concept of mobility control is that the displacing fluid mobility should be equal to or less than the (minimum) total mobility of displaced mul-

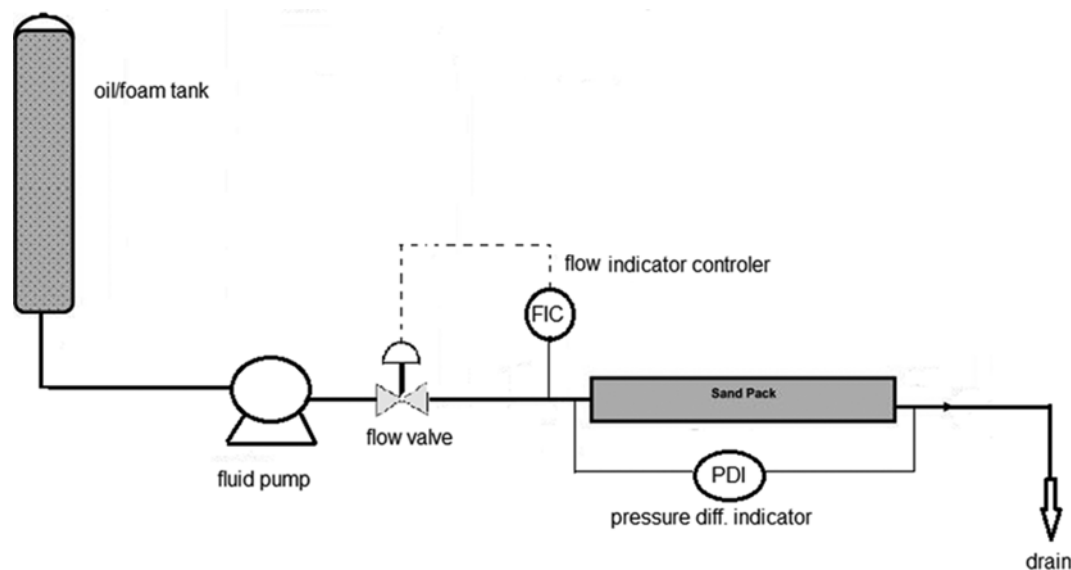


Fig. 9. A schematic diagram of the device for calculation of the mobility ratio.

tiphase fluids [19]. Accordingly, the following equipment was used to calculate the mobility control (see Fig. 9).

This equipment utilizes the Darcy formula.

$$Q = \frac{-K \cdot A \cdot \Delta P}{\mu \cdot L} \quad (2)$$

$$\lambda = \frac{Q \cdot L}{\Delta P \cdot A} \quad (3)$$

Then mobility ratio can be calculated as follows:

$$M = \frac{\lambda(\text{foam})}{\lambda(\text{oil})} \quad (4)$$

First, the desired fluids (crude oil and foam solution or formation brine water) were injected into the sand-pack holder with permeability of about 278 mD and flow rate of 10 mL/min. Afterwards, the production data, including produced oil and water and differential pressures were used to analyze the oil recovery and efficiency of the foam injection. A step-by-step calculation is given as follows for better clarification:

a) At first, mobility ratio of crude oil and formation brine water was calculated:

$$M = \frac{\lambda(B \cdot F \cdot \text{water})}{\lambda(\text{oil})} = \frac{0.282}{0.252} = 1.12 \quad (5)$$

b) Mobility ratio of crude oil and foam solution (1,000 ppm CTAB+ 750 ppm SiO<sub>2</sub> Nano-particle):

$$M = \frac{\lambda(\text{foam})}{\lambda(\text{oil})} = \frac{0.213}{0.252} = 0.845 \quad (6)$$

At the final stage, the obtained results were compared, which revealed that the water flooding resulted in fingering phenomenon or early breakthrough directly related to the mobility ratio. However, foam injection enhanced the mobility ratio in so that it could considerably enhance the oil recovery. In detail, based on the obtained

results, it can be deduced that the foam flooding in the gas injection or water flooding processes can control the mobility ratio in a manner that no fingering phenomenon, weak sweep efficiency, early breakthrough or early gas production (in gas injection process) would be observed.

## CONCLUSIONS

The effect of C<sub>19</sub>TAB and SiO<sub>2</sub> nanoparticles was investigated both on IFT reduction and foam stability using a systematic series of designed experiments. The performed experiments led to the following conclusions:

1. The obtained results revealed the significant role of SiO<sub>2</sub> nanoparticle on the stability of the produced foam. In detail, the foam of solutions prepared without nanoparticles disappeared after 90 min, while the solutions prepared using SiO<sub>2</sub> nanoparticles were stable for about 12 h.

2. IFT of foam solution/oil experienced a sharp reduction whenever surfactant concentration reached 1,000 ppm, while further increase in surfactant concentration led to a slight IFT reduction.

3. Addition of SiO<sub>2</sub> nanoparticles resulted in reduction of IFT values of the foam solution/oil with the highest reduction at concentration of 750 ppm.

4. Injected foam solution was capable to efficiently modify the mobility ratio between oil and foam solution from M=1.12 to M=0.845 (contained 1,000 ppm C<sub>19</sub>TAB surfactant+750 ppm SiO<sub>2</sub> nanoparticles), meaning that using foam injection as an efficient oil recovery process is feasible.

## NOMENCLATURE

A	: area of sand-pack
°API	: the american petroleum institute gravity
C <sub>19</sub> TAB	: hexa decyl trimethyl ammonium bromide
Ca	: calcium

Cl	: chloride
CMC	: critical micelle concentration
Cond.	: conductivity of formation brine water
D	: density
$D_e$	: diameter of pendant drop
EOR	: enhanced oil recovery
E.B.Water	: formation brine water
g	: acceleration of gravity
H	: a dependent parameter in the shape of drops
$\text{HCO}_3$	: bicarbonate
IFT	: interfacial tension
K	: permeability
L	: length
M	: mobility ratio
Mg	: magnesium
Na	: sodium
NaCl	: sodium chloride
Q	: flow
SDS	: sodium dodecyl sulfate
$\text{SiO}_2$	: silica di-oxide nano-particle
T.D.S	: total dissolved solids of formation brine water
WAG	: water alternating gas flooding
Wt%	: weight percent
$\Delta P$	: pressure differential
$\lambda$	: mobility
$\mu$	: viscosity
$\rho$	: density
$\sigma$	: interfacial tension

## REFERENCES

1. J. J. Sheng, *Pet. Sci. Eng. J.*, **120**, 216 (2014).
2. L. He, Y. Peng, L. Yan and W. Xin, *Acta Petrolei Sinica J.*, **31**, 91 (2010).
3. J. Zuta, I. Fjelde and R. Berenblyum, *SPE*, **129575** (2010).
4. J. S. Kim, Y. Dong and W. R. Rossen, *SPE*, **89351** (2004).
5. Q. Sun, Z. Li, S. Li, L. Jiang, J. Wang and P. Wang, *Energy Fuels*, **28**, 2384 (2014).
6. J. Yu, M. Khalil, N. Liu and R. Lee, *Fuel*, **126**, 104 (2014).
7. B. P. Binks, *Current Opinion in Colloid Interface Sci.*, **7**, 21 (2002).
8. M. I. Al-Mossawy, B. Demiral and D. M. A. Raja, *Int. J. Res. Reviews Appl. Sci.*, **7**, 4 (2011).
9. A. Worthen, H. Bagaria, Y. Chen, S. L. Bryant, C. Huh and K. P. Johnston, *SPE*, **154285** (2012).
10. T. Zhang, M. Roberts, S. L. Bryant and C. Huh, *SPE*, **121744** (2009).
11. M. Zargartalebi, R. Kharrat and N. Barati, *Fuel*, **143**, 21 (2015).
12. I. Kim, A. Taghavy, D. DiCarlo and C. Huh, *Petroleum Sci. Eng. J.*, **133**, 376 (2015).
13. Q. Sun, Z. Li, J. Wang, S. Li, B. Li, L. Jiang, H. Wang, Q. Lü, C. Zhang and W. Liu, *Colloids Surfaces A: Physicochem. Eng. Aspects*, **471**, 54 (2015).
14. M. Simjoo, T. Rezaei, A. Andrianov and P. L. J. Zitha, *Colloids Surfaces A: Physicochem. Eng. Aspects*, **438**, 148 (2013).
15. F. Moeini, H. Hemmati-Sarapardeh, M. H. Ghazanfari, M. Masihi and S. Ayatollahi, *Fluid Phase Equilib.*, **375**, 191 (2014).
16. A. Zolghadr, M. Escrochi and S. Ayatollahi, *J. Chem. Eng. Data*, **58**, 1168 (2013).
17. J. J. Sheng, *Modern chemical enhanced oil recovery (theory and practice)*, 241 (2011).
18. M. Lashkarbolooki, M. Riazi, F. Hajibagheri and Sh. Ayatollahi, *J. Mol. Liq.*, **216**, 377 (2016).
19. M. Lashkarbolooki, M. Riazi, S. Ayatollahi and A. Z. Hezave, *Fuel*, **165**, 75 (2013).
20. M. Lashkarbolooki and S. Ayatollahi, *Fluid Phase Equilib.*, **414**, 149 (2016).
21. M. Lashkarbolooki, S. Ayatollahi and M. Riazi, *J. Ind. Eng. Chem.*, **35**, 408 (2016).
22. J. J. Sheng, *Modern chemical enhanced oil recovery (theory and practice)*, 79 (2011).